PROTEIN MOTIFS

Protein folding creates structure-based, noncontiguous consensus phosphorylation motifs recognized by kinases

Mariana Lemos Duarte,[1]* Darlene Aparecida Pena,[1]* Felipe Augusto Nunes Ferraz,[2]* Denise Aparecida Berti,[1] Tiago José Paschoal Sobreira,[2] Helio Miranda Costa-Junior,[1] Munira Muhammad Abdel Baqui,[3] Marie-Hélène Disatnik,[4] José Xavier-Neto,[2] Paulo Sérgio Lopes de Oliveira,[2]† Deborah Schechtman[1]†

Linear consensus motifs are short contiguous sequences of residues within a protein that can form recognition modules for protein interaction or catalytic modification. Protein kinase specificity and the matching of kinases to substrates have been mostly defined by phosphorylation sites that occur in linear consensus motifs. However, phosphorylation can also occur within sequences that do not match known linear consensus motifs recognized by kinases and within flexible loops. We report the identification of Thr^{253} in α-tubulin as a site that is phosphorylated by protein kinase C βI (PKCβI). Thr^{253} is not part of a linear PKC consensus motif. Instead, Thr^{253} occurs within a region on the surface of α-tubulin that resembles a PKC phosphorylation site consensus motif formed by basic residues in different parts of the protein, which come together in the folded protein to form the recognition motif for PKCβI. Mutations of these basic residues decreased substrate phosphorylation, confirming the presence of this "structurally formed" consensus motif and its importance for the protein kinase–substrate interaction. Analysis of previously reported protein kinase A (PKA) and PKC substrates identified sites within structurally formed consensus motifs in many substrates of these two kinase families. Thus, the concept of consensus phosphorylation site motif needs to be expanded to include sites within these structurally formed consensus motifs.

INTRODUCTION

One reason that elucidation of signal transduction pathways is challenging is the difficulty in detecting and predicting specific targets for protein kinases. Among the factors that determine the recognition of a particular substrate by a specific protein kinase is the interaction of the catalytic site of the protein kinase with consensus sequences in the substrates. These consensus sequences are composed of amino acids flanking the phosphorylated residue. These residues often contribute to the specific recognition of the substrate by the protein kinase and aid substrate anchoring, increasing the interaction energy between the substrate and protein kinase, thereby favoring the formation of the complex (*1*). Within the consensus sequence, the phosphorylated residue on the substrate is referred to as P0 (the phosphorylation site), and the three residues flanking the phosphorylation site on the N and C-terminal sides are referred to as P−3, P−2, P−1 and P+1, P+2, and P+3, respectively. Subsites in the protein kinase that accommodate these seven residues of the peptide substrate are referred to as S−3, S−2, S−1, S0, S+1, S+2, and S+3. Interactions between substrates and protein kinases within these regions help determine protein kinase specificity and increase the interactions between protein kinases and their substrates. Structural modeling confirms that the amino acids flanking the phosphorylated residue are important for determining protein kinase specificity and increasing the interaction energy between a specific substrate and protein kinase (*2*).

Screens of peptide libraries for consensus motifs can predict protein kinase specificity (*3*–*5*), and phosphorylation sites are frequently predicted by inspecting primary amino acid sequences for linear consensus motifs (*6*). Computational methods are being used to understand the specificity of binding between substrates and protein kinases. Some of the strategies are based on the use of amino acid sequences of known substrates to identify conserved residues that would reveal a linear consensus motif (*7*, *8*). With this linear consensus motif in hand, similarity searches performed against databases of protein sequences predict substrate candidates. However, when the number of specific known substrates for the target kinase is low, establishing a linear consensus motif is difficult. Similarly, upon identification of previously unknown phosphorylation sites, protein kinases responsible for the phosphorylation events are commonly predicted on the basis of a linear consensus sequence containing the newly identified site (*6*).

Charge distribution (*9*) and frequency of disorder (*10*) have been suggested as important requisites for recognition of protein phosphorylation sites. Electrostatic interactions are likely involved in anchoring substrates to protein kinases, and these may be important for particular sets of kinases, such as the AGC family of kinases (*11*). However, overall differences in charge distribution cannot distinguish between substrates and nonsubstrates (*9*). On the basis of an increasing number of reported phosphorylation sites in databases and resolved structures, predictive tools that determine phosphorylation events using three-dimensional (3D) structures are emerging (*12*, *13*). For instance, DISPHOS uses information from disordered regions of the structures to predict the most probable phosphorylated residues (*10*), whereas NetPhos (*14*) groups the structures of substrates [available in the Protein Data Bank (PDB)] that were phosphorylated by similar kinases and structurally superimposes the substrates to predict new substrates on the basis of structural similarity. Another search for phosphorylation patterns involves calculating the relative frequencies of the 20 amino acids within radial distances ranging from 2 to 10 Å of the phosphorylated residue.

[1]Departamento de Bioquímica, Instituto de Química, Universidade de São Paulo, São Paulo 05508000, Brazil. [2]Laboratório Nacional de Biociências, Centro Nacional de Pesquisa em Energia e Materiais, Campinas 13083-970, Brazil. [3]Departamento de Biologia Celular e Molecular, Faculdade de Medicina de Ribeirão Preto, Universidade de São Paulo, Ribeirão Preto, São Paulo 14049-900, Brazil. [4]Department of Chemical and Systems Biology, Stanford University School of Medicine, Stanford, CA 94305, USA.
*These authors contributed equally to this work.
†Corresponding author. E-mails: deborah@iq.usp.br (D.S.); paulo.oliveira@lnbio.org.br (P.S.L.d.O.)

The most frequently occurring amino acids at these distances in substrates of specific protein kinases may contribute to kinase recognition (*12*, *15*). Screening surfaces for kinase interactions using docking methods is an uncommon approach to matching kinases with their substrates. Further knowledge on the nature of the 3D interaction between the kinase and its substrate can aid in the development of predictive tools.

With the advances in chemical biology (*16*), mass spectrometry (MS), and proteomics (*6*), new strategies have identified protein kinase–specific substrates in cells (*17*). Surprisingly, many substrates are phosphorylated on residues that are not within linear consensus motifs (*6*, *16*, *17*). Instead, the phosphorylated residues are often found in flexible structures, such as loops, which have been proposed to conformationally adapt to the catalytic site (*17*). Substrate docking sites in the kinase that are distant from the catalytic site are also important in enhancing substrate-kinase interactions (*18*, *19*).

Members of the protein kinase C (PKC) family of serine/threonine kinases recognize linear consensus motifs with basic residues (Lys or Arg) usually at the P-3 and P-2 positions (*20*). Indeed, a regulatory mechanism of the PKC family is the presence of a pseudosubstrate region within the enzyme's regulatory domain. This pseudosubstrate region contains an Ala rather than a phosphorylatable Ser or Thr at position P0 (*21*).

Pharmacological inhibition of PKC in embryonic stem cells decreases α-tubulin phosphorylation (*22*); however, whether this phosphorylation event is direct or indirect was not determined. Here, we reported that Thr^{253} of α-tubulin is a previously unknown PKC phosphorylation site. Thr^{253} is not present within a linear PKC consensus motif formed by flanking basic residues but rather has an acidic amino acid at position P-2. By analyzing structural models, we found that Thr^{253} is present within a "structurally formed" consensus motif in which basic residues (Lys^{163} and Lys^{164}) present in a distant part of the primary sequence are adjacent to the phosphorylation site in the folded protein, thereby producing a structurally formed PKC consensus motif. Mutation of these basic residues diminished α-tubulin phosphorylation at Thr^{253} by PKCβI. Previous studies reported that phosphorylated PKC is found at the mitotic spindle of mouse eggs (*23*). Here, we determined that PKCβI localized at the mitotic spindle of HeLa cells and that phosphorylation of α-tubulin at Thr^{253} occurred in dividing cells.

Like PKC, protein kinase A (PKA) also recognizes phosphorylation sites preceded by basic residues (*4*). By inspecting previously reported PKA or PKC substrates that do not contain linear consensus motifs and by performing molecular docking simulations, we found that phosphorylated sites within structurally formed consensus motifs were also predicted to exist in these substrates: In the folded protein substrates, basic residues distant in the linear sequence come close to the phosphorylated residue and were predicted to interact with residues in the protein kinase, thus promoting a functional interaction between the substrate and the kinase. Our results showed that structurally formed consensus motifs are common and that analysis of linear sequences surrounding phosphorylation sites may reveal only a subset of substrates.

RESULTS

PKC phosphorylates α-tubulin in a site that is not part of a linear consensus motif

α-Tubulin is a highly conserved protein (99.3% identical among 12 vertebrate species), and residue Thr^{253} is among the conserved amino acids (fig. S1). We performed an in vitro protein kinase assay with recombinant rat PKCβI and α-tubulin purified from bovine brain to determine whether α-tubulin was a substrate of PKC. MS analysis of the in vitro kinase reactions indicated that Thr^{253} was phosphorylated by PKCβI (Fig. 1A). To investigate Thr^{253} phosphorylation by PKC in cellular contexts, we generated polyclonal antibodies against a linear peptide, containing the sequence surrounding phosphorylated Thr^{253} in α-tubulin (Fig. 1B). Serum from one mouse (animal 4) [anti–p-α-tubulin (Thr^{253})] had the best relative response for the phosphorylated peptide containing $pThr^{253}$ (Fig. 1B) and was used for subsequent experiments. In Western blots, anti–p-α-tubulin (Thr^{253}) was significantly more effective at recognizing purified α-tubulin

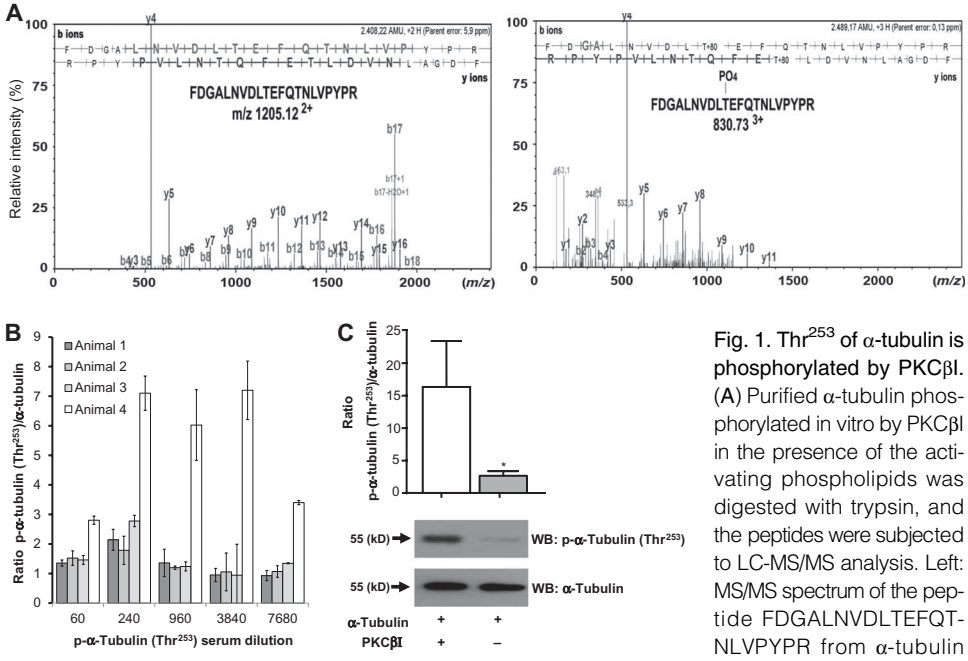

Fig. 1. Thr^{253} of α-tubulin is phosphorylated by PKCβI. (**A**) Purified α-tubulin phosphorylated in vitro by PKCβI in the presence of the activating phospholipids was digested with trypsin, and the peptides were subjected to LC-MS/MS analysis. Left: MS/MS spectrum of the peptide FDGALNVDLTEFQTNLVPYPR from α-tubulin without phosphorylation modification (monoisotopic mass of the unprotonated peptide = 2408.22 daltons). Right: MS/MS spectrum of the same peptide with phosphorylation in Thr^{253} (monoisotopic mass of the unprotonated peptide = 2489.17 daltons). (**B**) Recognition of the phosphorylated peptide (GALNVDLpTEFQTNLVP) relative to the nonphosphorylated peptide by antibodies in serum from mice immunized with the phosphorylated peptide. Peptide binding was detected by enzyme-linked immunosorbent assay (ELISA). (**C**) In vitro phosphorylation of purified α-tubulin by PKCβI detected by Western blot analysis with an antibody recognizing α-tubulin or the serum from animal 4 recognizing p-α-tubulin (Thr^{253}). Equal amounts of PKCβI-phosphorylated α-tubulin were loaded on separate gels and reacted with either anti–p-α-tubulin (Thr^{253}) or the antibody recognizing α-tubulin. Quantified data from three independent experiments shown as mean and SD are shown along with representative blots. Statistical significance was determined using Mann-Whitney test; $^*P = 0.0286$.

phosphorylated in vitro by PKCβI than nonphosphorylated α-tubulin (Fig. 1C). The phosphorylated peptide also blocked anti–p-α-tubulin (Thr^{253}) from recognizing PKCβI-phosphorylated α-tubulin more effectively than did the nonphosphorylated peptide (fig. S2). The MS data indicated that the phosphorylated Thr is not flanked by basic amino acids commonly found in PKA (*20*) and PKC (*4*) consensus site motifs (R/K R/K X S/T), but rather by an acidic Asp (D) at position P-2 (Fig. 1A).

α-Tubulin contains a structurally formed PKC consensus motif

Using the structure of *Bos taurus* (PDB ID: 1JFF) (*24*), we identified the location of the phosphorylated Thr^{253} and found that Lys^{163} and Lys^{164}, which are also conserved in several vertebrates (fig. S1), were spatially close to the phosphorylated site (Fig. 2A). The distance between the α carbon (Cα) of Lys^{164} and Cα of Thr^{253} is 8.12 Å. The structure of PKI, a peptide inhibitor of PKA (PDB ID: 1FMO) (*25*), has a similar distance; the distance between Cα of Arg^{19} and Cα of Ala^{21} in PKI is 6.61 Å (Fig. 2A).

To understand at the molecular level how PKCβI may recognize this phosphorylation site in α-tubulin, we modeled the interaction between α-tubulin and PKCβI (Fig. 2, B and C), setting Lys^{163} as P-3, Lys^{164} as P-2, and Thr^{253} as P0 (see Materials and Methods for the details of the modeling and models S1). Comparison of the interaction of the refined protein kinase model containing the PKI peptide (representing a linear consensus motif) with the structurally formed consensus motif of α-tubulin considering these three key residues of α-tubulin (P-3, P-2, and P0) relative to PKI produced low root mean square deviation (RMSD) values (Table 1), indicating that the structure and the model were similar. Molecular modeling and docking thus suggested that Lys^{163} and Lys^{164} could functionally substitute for basic residues in a linear PKC consensus motif, anchoring α-tubulin to PKC.

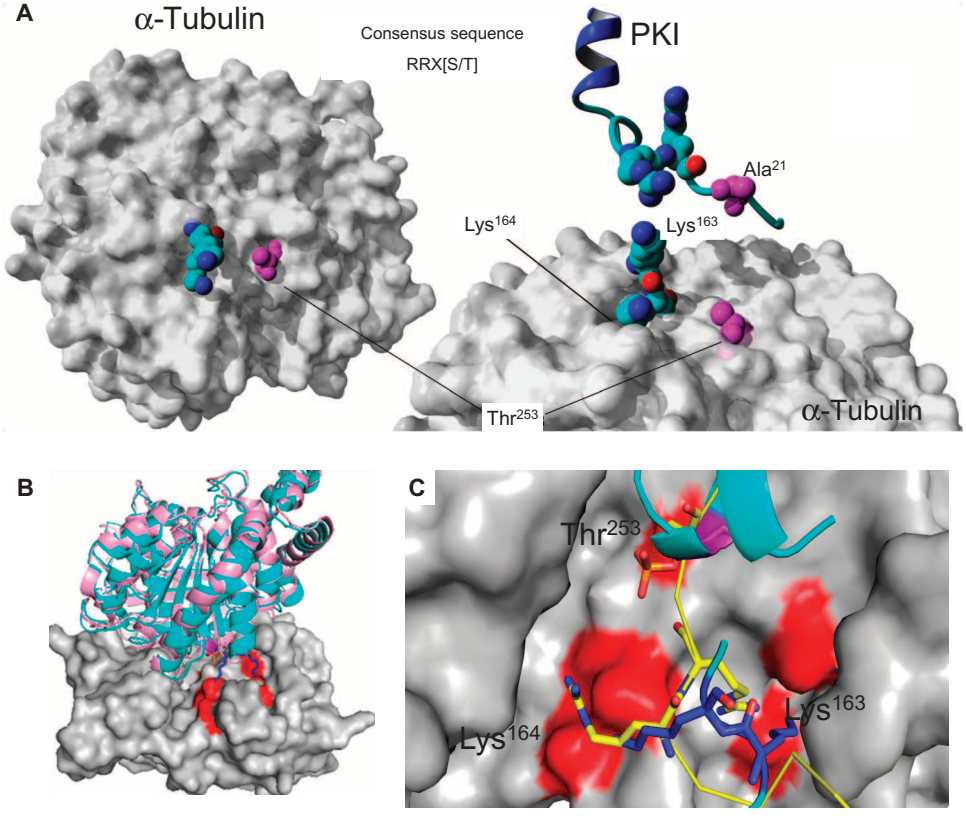

Fig. 2. Analyses of the structurally formed PKC consensus motif containing Thr^{253} in α-tubulin. (A) Comparison of PKI, representing a linear consensus motif, and the structurally formed consensus motif comprising Lys^{163}, Lys^{164}, and Thr^{253}. In sphere representation, residues suitable to act as P0 (Thr^{253} on α-tubulin and Ala^{21} on PKI) are pink. Anchoring residues (Lys^{163} and Lys^{164} on α-tubulin and Arg^{18} and Arg^{19} on PKI) are blue. (B) Proposed model for the α-tubulin and PKC complex. PKC is shown in gray, with acid residues forming the S-3, S-2, and S0 substrate interaction regions in red. Docked α-tubulin is shown in cyan cartoon representation, with the anchoring residues (Lys^{163} and Lys^{164}) represented in blue sticks and the phosphorylated Thr^{253} in purple. The nondocked original structure of α-tubulin of *B. taurus* [PDB ID: 1JFF] (*24*) is shown in pink and aligned over the docked one for conformational change comparison. (C) Enlarged image of the interaction region on the docked model shown in (B), with PKI (yellow) for positional reference. Key residues on PKI are represented as sticks (yellow). Blue and pink residues in stick are the key residues on α-tubulin.

Phosphorylated sites are present in structurally formed consensus motifs in multiple PKC and PKA substrates

Analysis of the PhosphositePlus database demonstrated that of 1095 PKA substrates, 140 lack a linear consensus motif for PKA: a basic amino acid at either P-3 or P-2. Of the 140 substrates that did not contain a linear consensus motif, we generated 27 substrate homology models containing 36 nonlinear consensus motifs (table S1). Among these, we used 33 structurally formed consensus motifs to simulate the interaction with PKA. Three of the phosphorylation sites modeled did not display anchoring basic residues: T^{19} and S^{20} on Q64122 had basic residues in regions that could not be modeled, and S^{182} on P11473 did not have anchoring residues. Three representative substrates with two basic residues as anchors and low local RMSD (modeled substrate relative to docked substrate) are shown (Fig. 3 and models S1). Also, three different substrates each with a linear consensus motif were modeled (table S1 and models S1).

Microtubule-associated protein light chain 3 (LC3), a PKA and PKC substrate, has phosphorylated Thr^{29} (P0) (*26*) and anchoring basic residues Arg^{24} (P-2) and Arg^{21} (P-3) (Fig. 3A). Regulator of G protein (heterotrimeric guanine nucleotide–binding protein) signaling (RGS13) (*27*) is phosphorylated by PKA and has phosphorylated Thr^{41} (P0) and anchoring residues Arg^{18} (P-2) and Lys^{17} (P-3) (Fig. 3B). Death-associated protein 3 (DAP3) (*28*) is also phosphorylated by PKA and has phosphorylated Ser^{185} (P0) and anchoring residues Lys^{192} and Lys^{189} (Fig. 3C). We aligned the structural consensus with the peptide from PKI, which is a linear consensus motif, to compare the interaction

Table 1. RMSD calculation for PKA-docked models with structurally formed consensus sites, compared to the linear peptide from PKI and the nondocked substrate model. Substrates were divided into two different groups: α-tubulin (Thr^{253}) and phosphorylated sites without a linear consensus motif as obtained from PhosphositePlus data bank and shown in Fig. 3. The docked substrate represents the model of the substrate docked with PKA and the nondocked substrate starting model, derived from the published crystal structure (table S1). RMSD values are shown for comparisons of the PKA-docked modeled substrate and modeled nondocked substrate (whole substrate), the 10 residues flanking each side of the phosphorylated residue (p-residue) in the docked and nondocked models, the 10 residues flanking each side of the pair of anchoring residues in docked and nondocked models, and the p-site and anchor residues in the docked models (key residues) compared to the analogous key residues in PKI (P0, P-2, and P-3). For the comparison of the key residues, only Cα, Cβ, and Cγ when present in the p-site and anchor residues in the substrate were used.

Models	Protein	p-Site	Anchors	Docked and nondocked substrates (Å)			Key residues and PKI
				Whole substrate	Ten residues around the p-residue	Ten residues around anchoring residues	
Tubulin	α-Tubulin	T^{253}	K^{165}, K^{164}	1.16	2.27	3.18	1.83
Lacking a linear consensus motif	LC3	T^{29}	R^{21}, R^{24}	0.77	1.72	1.66	2.08
	RGS13	T^{41}	K^{17}, R^{18}	1.55	2.81	3.70	2.38
	DAP3	S^{185}	K^{189}, K^{192}	1.63	1.93	3.60	2.72

of the kinase with PKI peptide to that of the kinase with the structurally formed consensus motif in LC3, RGS13, and DAP3 (Table 1). RMSD values of PKI and the key residues of the substrates docked with PKA are low, indicating that other substrates besides α-tubulin can adopt a structure similar to a linear consensus sequence. The modeled substrate structures docked to kinase structures were not substantially different than the nondocked substrate structures as determined by RMSD values obtained from comparing the PKA-docked models and nondocked models of the substrates in the regions that interact with the protein kinase (*17*–*19*) (Table 1). We performed the same type of analysis with substrates containing linear PKA consensus motifs docked to PKA (fig. S3, A to F), which produced RMSD values relative to PKI that were less than 1 (table S2). These data indicated that the docking process did not cause structural disruption in either the structures of the kinase or the substrate.

Anchoring residues Lys^{163} and Lys^{164} are key for Thr^{253} phosphorylation by PKCβI

We created a fusion protein between green fluorescent protein (GFP) and α-tubulin (GFP-α-tubulin) to assess the importance of the structurally formed consensus motif in α-tubulin for phosphorylation by PKC and function in cells. We individually mutated Lys^{163} and Lys^{164} to alanine in GFP-α-tubulin to confirm that these residues are necessary for PKC phosphorylation of α-tubulin. As a control, we also generated a T253A mutant. When expressed in HeLa cells, the GFP-α-tubulin proteins, including the T253A, K163A, and K164A mutants,

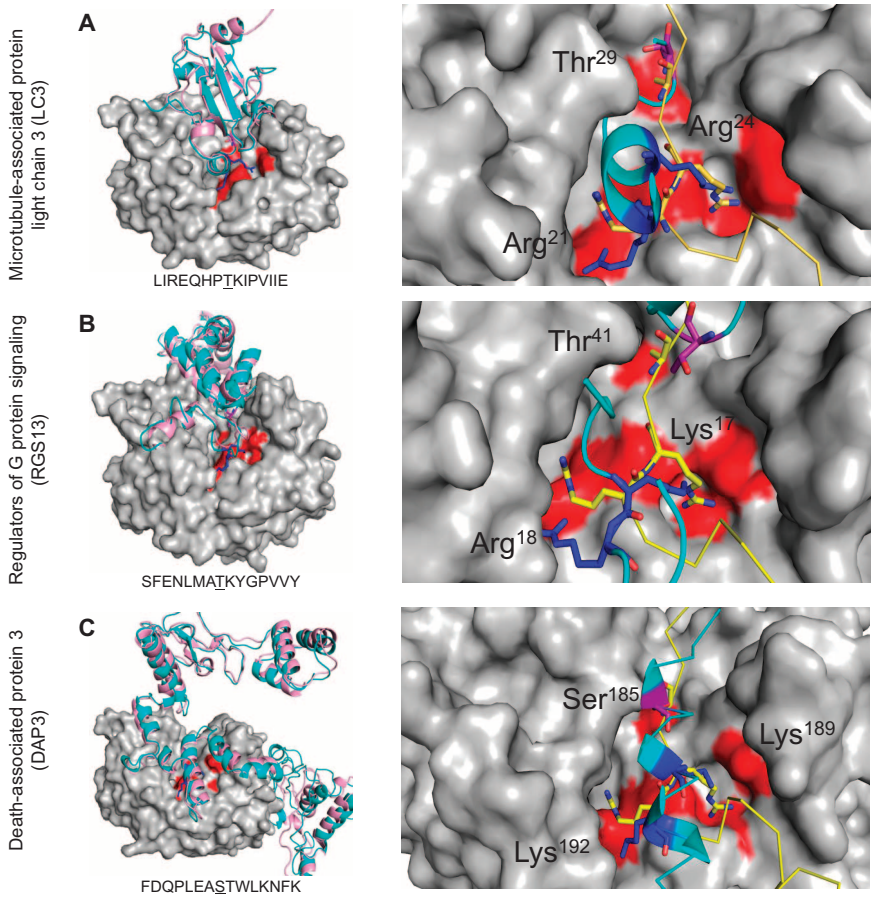

Fig. 3. Three models of known PKA substrates that could use structurally formed consensus motifs to interact with PKA. (A to C) Modeled PKA substrates containing structurally formed consensus motifs: LC3 (A), RGS13 (B), and DAP3 (C). Linear sequences flanking the phosphorylated site (p) obtained from PhosphositePlus data bank are displayed. Left: PKA is shown in gray, with acid residues forming the S-3, S-2, and S0 substrate interaction regions in red; the docked substrates are shown in cyan cartoon representation, with interacting residues represented as sticks in blue and the phosphorylated residue in purple stick. The original structure of the substrate aligned over the docked one is shown in pink. Right: Enlarged images of the interaction region on the docked models, with PKI (yellow) for positional reference. Labels identify the key residues (phosphorylated site and anchor residues) on the substrate.

were incorporated into tubulin fibers (Fig. 4A). To assess the importance of the key residues for PKC-mediated phosphorylation, we immunoprecipitated the GFP-α-tubulin wild type and mutants from human embryonic kidney (HEK) 293T cells with an antibody recognizing GFP and then used the immunoprecipitated proteins for in vitro kinase assays with recombinant rat PKCβI. Anti–p-α-tubulin (Thr^{253}) detected phosphorylated α-tubulin in wild-type GFP-α-tubulin (Fig. 4B). However, phosphorylation was undetectable for the T253A mutant and was significantly decreased by mutation of either Lys^{163} or Lys^{164}, confirming the importance of these lysine residues for Thr^{253} phosphorylation by PKCβI (Fig. 4).

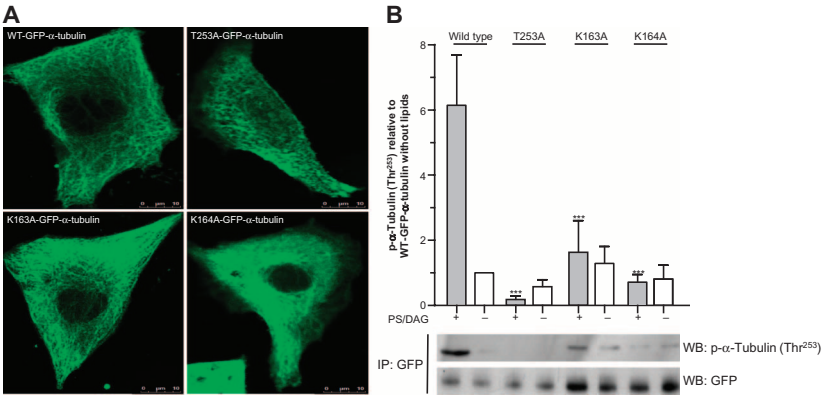

Fig. 4. Lys^{163} and Lys^{164} contribute to PKC phosphorylation of α-tubulin. (A) HeLa cells were transfected with the indicated GFP-α-tubulin constructs. Fixed cells were stained with the antiserum recognizing GFP, and fluorescence was detected by confocal microscopy. Images are representative of all cells that were GFP-positive. (B) Immunoprecipitated GFP-α-tubulin proteins from transfected HEK 293T cells were phosphorylated by PKCβI in vitro. Samples were analyzed by Western blotting with the antibodies or serum recognizing p-α-tubulin (Thr^{253}) or α-tubulin. The amount of GFP-α-tubulin immunoprecipitated was determined by running 10% of the reaction on a separate gel and blotting with an antibody recognizing GFP. A representative experiment ($n = 3$) is shown. The graph showing the average and SD indicates the amount of p-α-tubulin (Thr^{253}) relative to the amount detected with anti–p-α-tubulin (Thr^{253}) in assays with the kinase and wild-type (WT) GFP-α-tubulin in the absence of lipids. Statistical analysis was performed using two-way analysis of variance (ANOVA); $^{***}P < 0.01$.

α-Tubulin Thr^{253} phosphorylation occurs in cells during mitosis

Direct protein substrates have to physically interact with protein kinases in the context of living cells. We found that PKCβI localized mainly at the mitotic spindle during different stages of cell division in HeLa cells (Fig. 5, A and B). In particular, PKCβI accumulated on the spindle of cells in the later stages of mitosis. Similarly, staining cells with anti–p-α-tubulin (Thr^{253}) indicated that phosphorylation of Thr^{253} occurred mainly at the mitotic spindle (Fig. 5C). Exposing HeLa cells to Gö 6983, a general PKC inhibitor, significantly decreased α-tubulin phosphorylation at Thr^{253} detected by Western blot with anti–p-α-tubulin (Thr^{253}), providing additional support for PKC-mediated phosphorylation of this site on α-tubulin in cells (Fig. 5D).

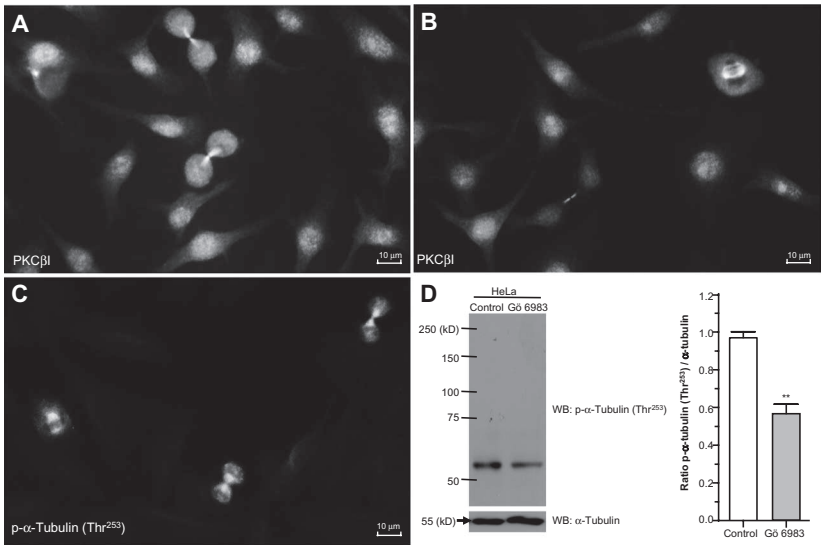

Fig. 5. PKCβI Thr^{253} phosphorylation is enriched at the mitotic spindles. (A and B) PKCβI detected at the mitotic spindle in HeLa cells at different stages of cell division. (C) Phosphorylated α-tubulin (Thr^{253}) detected in dividing HeLa cells with anti–p-α-tubulin (Thr^{253}). (D) Effect of inhibition of PKC on α-tubulin Thr^{253} phosphorylation in HeLa cells exposed to 10 μM Gö 6983 for 6 hours. Lysates were assayed by Western blot by probing for p-α-tubulin (Thr^{253}) and α-tubulin. The plot shows the average and SD of the ratio between p-α-tubulin (Thr^{253}) and α-tubulin ($n = 3$). Blots from a representative experiment are also shown. Statistical analysis was determined using the nonparametric Mann-Whitney test; $^{**}P < 0.05$.

DISCUSSION

Few PKC substrates have been experimentally identified thus far, which relates to difficulties imposed by the biological complexity of these kinases and the low abundance of some of the substrates. The computational strategies commonly used to identify PKC targets search for linear PKC consensus motifs (*29*), despite reports of many protein kinase substrates that lack linear consensus motifs (*17*). Here, our results demonstrated that the strategy of looking for phosphorylation sites only within linear consensus motifs may exclude several substrates.

We identified a previously unknown PKC phosphorylation site in α-tubulin, Thr^{253}. This site is present within a motif formed by residues that, although placed at distant parts of the primary sequence, in the folded protein are arranged such that they mimic the recognition sequence of a linear consensus motif–containing peptide. This PKC phosphorylation site and others that are part of structurally formed consensus motifs cannot be identified by searching for linear PKC consensus motifs composed of basic residues flanking the phosphorylated residue. Indeed, in the linear sequence containing Thr^{253} at P-2, there is a negatively charged Asp, which is incompatible with the electrostatic requirements of a PKC substrate. Furthermore, inspection of the 3D structure of α-tubulin showed that basic residues Lys^{163} and Lys^{164} are in close proximity to Thr^{253} and that, structurally, this environment resembles the PKA peptide inhibitor, PKI, which contains a linear PKA/C consensus motif (*25*). We detected PKCβI and Thr^{253}-phosphorylated α-tubulin at the mitotic spindle in dividing cells, and pharmacological inhibition of PKC in HeLa cells decreased Thr^{253} phosphorylation, which is consistent with another study that also reported phosphorylation of Thr^{253} in α-tubulin of synchronized HeLa cells (*6*). Thus, this phosphorylation

event occurs in cells during mitosis. Future studies need to evaluate the physiological importance of this phosphorylation.

Phosphorylation in flexible regions that would adapt to fit into the catalytic site of a kinase has been suggested as a reason for phosphorylation occurring in the absence of a linear consensus motif (*17*). However, comprehensive structural analysis of experimentally identified phosphorylation sites demonstrated that 37% of the phosphorylation sites mapped to protein regions displaying a well-defined secondary structure (*13*).

In addition to promoting the binding of the substrate to the catalytic site, substrate docking sites located at a distance from the catalytic site are also important for defining substrate specificity (*18*, *19*). On the basis of the structure of the kinase domain (*2*) and analysis of phosphorylated substrates deposited in databases (*15*), researchers have suggested that kinases could recognize substrates in a structural manner. Indeed, our data validated the importance of consensus sequences in substrate binding to protein kinases and extended this notion by showing that tertiary structure contributes to structurally formed consensus motifs. Therefore, both linear consensus motifs and structurally formed consensus motifs should be considered when analyzing and predicting protein kinase phosphorylation sites.

Our data indicate that phosphorylation events could be mediated by recognition of a structurally formed consensus motif. Because usually protein kinases interact with substrates in a very similar fashion and substrates can be phosphorylated on sites not within linear consensus motifs, we expect that the recognition of substrates with structurally formed consensus motif extends beyond the PKC and PKA families.

MATERIALS AND METHODS

Cell culture

HEK 293T cells, obtained from B. Malnic (University of São Paulo, Instituto de Química), and HeLa cells, obtained from R. Tonelli (Federal University of São Paulo), were maintained in high-glucose Dulbecco's modified Eagle's medium (DMEM) supplemented with 10% fetal calf serum and penicillin/streptomycin (Gibco-BRL) at 37°C under 5% CO_2.

In vitro phosphorylation of α-tubulin and identification of the phosphorylated residue

Purified bovine tubulin (TL238, Cytoskeleton) was phosphorylated in vitro with rat recombinant PKCβI (Santa Cruz Biotechnology) as previously described (*30*) but without [^{32}P]adenosine triphosphate (ATP). The phosphorylation site was identified by liquid chromatography–tandem MS (LC-MS/MS) performed at Stanford University MS facility (https://mass-spec.stanford.edu/). Phosphorylated protein was precipitated with 4 volumes of −80°C acetone. Protein pellets were reconstituted in 15 μl of 8 M urea (pH 7.8) and 20 μl of 0.2% Protease Max (Promega) per manufacturer's protocol. Samples were solubilized by shaking and sonication at room temperature. Solubilized material was reduced for a half hour at 55°C using dithiothreitol (5 mM); samples were cooled to room temperature, alkylated with iodoacetamide [10 mM and 0.1 μg of sequencing-grade trypsin (Promega)], and digested overnight at 37°C. Samples were then acidified with formic acid and purified using in-house packed STAGE tips.

For LC-MS/MS analysis and identification of phosphorylated residues, liquid chromatography was done using Eksigent nano2D LC coupled to an in-house packed C18 analytical column. A Michrom source was used for nano–electrospray ionization at a flow rate of 750 nl/min. A 1-hour linear gradient from 2% mobile phase B (acetonitrile with 0.1% formic acid) to 40% B was used. Data were acquired using an LTQ Orbitrap Velos mass spectrometer (Thermo Fisher) in a data-dependent fashion (MS/MS via higher-energy C-trap dissociation) of the top 10 most intense precursor ions. RAW files were converted to mzXML format and searched on a Sorcerer (SageN) processing system using Sequest against the appropriate SwissProt and NCBI (National Center for Biotechnology Information) databases. Search results were uploaded into a Scaffold workstation.

Generation and characterization of antibodies recognizing p-α-tubulin (Thr^{253})

Mice were immunized with p-α-tubulin (Thr^{253}) peptides obtained from Proteimax. Coupling of both phosphorylated (GALNVDLp**T**EFQTNLVP) and nonphosphorylated (GALNVDLTEFQTNLVP) peptides to keyhole limpet hemocyanin (KLH) (Sigma-Aldrich) or to bovine serum albumin (BSA) was performed with formaldehyde according to the manufacturer's instruction. We immunized four 8-week-old female BALB/c mice from Biotério de Produção e Experimentação da Faculdade de Ciências Farmacêuticas e do Instituto de Química da USP (housed according to the specifications of the *Guide for the Care and Use of Laboratory Animals*). Emulsion of the phosphorylated peptide coupled to KLH (50 μg) and complete Freund's adjuvant was administered intraperitoneally, followed by three booster immunizations at 7-day intervals with the emulsion prepared using incomplete Freund's adjuvant. Pre- and postimmunization blood samples were collected, and the antibody titer was determined by ELISA. One hundred microliters of nonphosphorylated or phosphorylated peptide coupled to BSA (100 ng peptide, assuming that all 2.5 mg of peptide efficiently coupled to 5 mg BSA) diluted in phosphate-buffered saline (PBS; pH 7.4) was added to each well of 96-well ELISA plates and incubated overnight at 4°C. Plates were washed three times with PBS plus 0.05% Tween 20 (PBS/Tween) and blocked with 5% nonfat milk in PBS for 1 hour at 37°C. After the addition of 100 μl of serial serum dilutions, the plates were incubated for 2 hours at 37°C, then washed three times with PBS/Tween. After the addition of 100 μl of horseradish peroxidase–conjugated goat anti-mouse immunoglobulin G (Sigma-Aldrich), the plates were incubated for 1 hour at 37°C and washed three times in PBS/Tween; 100 μl of TMB (3,3′,5,5′-tetramethylbenzidine) substrate (BD Biosciences) was subsequently added, and absorbance was read at 655 nm. To identify the serum that best differentially recognized the phosphorylated peptide, we calculated the ratio of the absorbance in the presence of the nonphosphorylated to that in the presence of the phosphorylated peptide, and the serum from a mouse that recognized the phosphorylated peptide at lower dilutions than those required to detect the nonphosphorylated peptide [anti–p-α-tubulin (Thr^{253})] was determined and used for Western blot and immunofluorescence experiments at 1:1000 and 1:100, respectively. The specificity of anti–p-α-tubulin (Thr^{253}) was evaluated by preadsorption of this antibody with 100 μM immunization peptide containing a phosphorylated Thr^{253} or the nonphosphorylated peptide. After 2 hours of incubation at 37°C, blocked antibodies were used in Western blot assays with in vitro PKC-phosphorylated α-tubulin.

Docking, structural alignments, alignments, energy minimization, and molecular dynamics

To explore the effects of 3D structure surrounding the phosphorylation sites in proteins, we obtained validated PKA substrates from the phosphorylation data bank PhosphositePlus (search performed on 2 July 2014). We chose PKA substrates because the crystal structure of this protein kinase has been solved in complex with the inhibitor peptide PKI (PDB ID: 1FMO) (*25*), which we used as reference to model all kinase-substrate interactions. All substrate structures were generated through homology modeling using YASARA software (*31*). A geometrical search was performed on all the substrates, taking as starting reference the residue known to be phosphorylated and searching for exposed residues matching the phosphorylation motif,

which we considered to be basic residues within 14 Å of the phosphorylated residue. Distance restrictions were made on the basis of the structure of PKI. An initial kinase-substrate complex model was made by aligning key residues on the protein over the P0 and P-2 onto the structure of PKI in complex with PKA. We moved this initial model by rotating the protein kinase on the vector defined by the Cα of these residues, searching for the conformation that minimized atom overlaps. All the structural alignments for model generation and RMSD calculations were made using YASARA (*31*).

Models that presented a possible structural phosphorylation motif were refined through steered energy minimization. Taking as starting point the noninteracting (independent or unbound) structures of the kinase and the substrate, we tried to achieve the conformation created by overlapping the key residues of the substrate onto PKI. The low-energy pathway between the two conformations was calculated with YASARA through a restrained simulated annealing minimization. We applied a force of 25 pN pointing toward the target coordinates to all atoms. We then evaluated the final model by comparing the docked and nondocked structures. The energy minimization used YAMBER3 force field (*31*). This steered docking process was used to evaluate whether the region of the substrate containing the phosphorylated residue can access and interact with the binding site of the protein kinase without hindrance or requiring large conformational changes to both structures. Changes in the structures were evaluated by calculating the global and local (around the key residues) RMSD values relative to the structure of the starting model of the substrate.

To generate images, we refined the models using a steered molecular simulation that included springs connecting the side chains of key residues of the substrate protein, the ones proposed to act as anchors and the phosphorylated residue, with residues forming the subsites, the substrate docking residues in the kinase. Connections were made using springs with a stretching constant of 30 N/m and an equilibrium length of 3.5 Å. Atoms on the backbone of the protein kinase were fixed, forcing only the substrate structure to adjust to the docking conformation, and the dynamics ran until the springs reached the equilibrium state. Subsite residues on PKA were extracted from the literature: Tyr^{330} and Glu^{127} for S-3; Glu^{230}, Tyr^{204}, Glu^{203}, Thr^{201}, and Glu^{170} for S-2; and Asp^{166} for S0 (*2*).

To generate the α-tubulin–PKC complex, we followed the same process described above, using the α-tubulin structure of *B. taurus* (PDB ID: 1JFF) (*24*) as the substrate and a PKCβI structure built through homology modeling, on the basis of the sequence of the protein kinase domain of a rat PKCβI (UniProt: P68403, CDD: 214567) using [PDB ID: 1FMO (*25*)] as template. The template presented a coverage of 96.1% and an identity of 43.8%. Alignment of the PKA and PKC sequences was performed using Clustal X (*32*), and the analogous residues forming subsites on the PKC structure were determined.

Plasmids and site-directed mutagenesis

Human α-tubulin from the GFP-α-tubulin vector (Evrogen) was subcloned into the mammalian expression vector pEGFP-CI (Clontech) between the restriction enzyme sites Xho I and Bam HI. Site-directed mutagenesis was performed using the Stratagene QuikChange kit according to the manufacturer's instructions. Primers for construction of the mutants were as follows: T253A mutation forward 5′-TGAATGTTGACCTGGCAGAATTCCAGACCAAC-3′ and reverse 5′-GTTGGTCTGGAATTCTGCCAGGTCAACATTCA-3′; K163A mutation forward 5′-GTTGATTATGGCGCGAAGTCCAAGCTGGAGT-3′ and reverse 5′-ACTCCAGCTTGGACTTCGCGCCATAATCAAC-3′; K164A mutation forward 5′-GTTGATTATGGCAAGGCGTCCAAGCTGGAGT-3′ and reverse 5′-ACTCCAGCTTGGACGCCTTGCCATAATCAAC-3′. Selected clones were sequenced with BigDye Terminator v3.1 Cycle Sequencing Kits (Life Technologies) at the sequencing facility at Universidade de São Paulo, Instituto de Química with an ABI 3730 DNA Analyzer. DNA from clones containing the specific desired mutations was prepared using a Qiagen Midi Prep kit.

Transfection of HeLa and HEK 293T cells

Transfections were performed using Lipofectamine 2000 (Invitrogen) according to the manufacturer's instructions. For immunofluorescence studies, HeLa cells were transfected for 48 hours, then fixed with 4% paraformaldehyde, and labeled with an antibody recognizing GFP as described below.

Immunoprecipitation of GFP-α-tubulin and in vitro phosphorylation

For immunoprecipitation assays, HEK 293T cells were used; 1 μl of antiserum against GFP (*33*), donated by F. Gueiros Filho (University of São Paulo, Instituto de Química), was incubated with 50 μl of packed volume of protein G beads (Invitrogen) for 2 hours at 4°C. Antibody-bound beads were then washed twice with PBS and blocked with 1% BSA for 1 hour at 4°C. Cells transfected with GFP-α-tubulin or the three mutants were lysed in PBS (pH 7.4) containing both protease inhibitor cocktail (Sigma-Aldrich) and phosphatase inhibitor cocktail PhosStop (Roche) by three freeze-thaw cycles. Cells were then sonicated for 30 min at 80 Hz (output) with a probe sonicator (Branson Sonifier 250). Cell lysates were precleared with protein G beads for 1 hour at 4°C, incubated with antibody-bound beads overnight at 4°C, and subsequently washed with PBS. Bound proteins were used in phosphorylation assays with PKCβI. Immunoprecipitated proteins were mixed with 80 ng of PKCβI, 40 μM ATP, 40 mM $MgCl_2$, 2 mM $CaCl_2$, phosphatidylserine (PS; 60 μg/ml), dioleoylglycerol (DG; 2 μl/ml) in 20 mM tris-HCl (pH 7.4) at 37°C for 20 min. The reactions were stopped by addition of Laemmli buffer. Phosphorylated immunoprecipitates were analyzed on two different 10% SDS–polyacrylamide gel electrophoresis (SDS-PAGE), one in which 15% of the immunoprecipitated amount was transferred and probed for GFP and the other 75% was transferred and probed with anti–p-α-tubulin (Thr^{253}). Densitometric analyses were performed with ImageJ. The GFP signal was used to normalize the amount of transfected immunoprecipitated GFP-α-tubulin. Because transfection efficiency varied for each construct, normalization was performed separately for each construct. Bands were quantified, and the ratio of p-α-tubulin (Thr^{253}) to α-tubulin in immunoprecipitates of the wild-type GFP-α-tubulin without the PKC activators $CaCl_2$, PS, and DG was determined for each construct. Statistical analysis was performed on data from at least three experiments using two-way ANOVA.

Immunofluorescence

For immunofluorescence studies, cells were cultured on 13-mm glass coverslips coated with 3% gelatin. Cells at 80% confluence were fixed with 4% paraformaldehyde, permeabilized with PBS–0.1% Triton X-100, and blocked in blocking solution (PBS, 0.1% Triton X-100, 1% normal goat serum) for 40 min at room temperature in a humidified chamber. Cells were incubated overnight at 4°C in a humidified chamber with a mouse antibody recognizing PKCβI (sc-8049, Santa Cruz Biotechnology), at a final concentration of 2 μg/ml, or the serum with anti–p-α-tubulin-Thr^{253} diluted 1:100 in blocking solution, or with rabbit anti-GFP serum (1:1000), followed by incubation in the dark for 1 hour at room temperature with goat anti-mouse conjugated with Alexa 555 (4 μg/ml) or goat anti-rabbit conjugated with Alexa 488 (4 μg/ml). Immunofluorescence staining was analyzed using a fluorescence microscope (Nikon Eclipse E600).

Transfected cells were labeled with the antibody recognizing GFP, diluted 1:1000, and visualized by Alexa 488–conjugated goat anti-rabbit (Molecular Probes) (8 μg/ml) diluted in blocking solution. Fluorescence was detected using a Leica TCS SP5 laser scanning confocal microscope (Leica Microsystems) in Laboratório de Microscopia Confocal, FMRP-USP.

Inhibition of PKC in cells

HeLa cells were plated in high-glucose DMEM containing 10% fetal bovine serum (FBS), and 24 hours after plating, medium was changed to serum-free DMEM to partially synchronize the cells. After serum starvation for 24 hours, cells were released into cell cycle by the addition of 10% FBS and then incubated in the presence or absence of 10 μM Gö 6983 (Sigma-Aldrich) for 6 hours. Lysates were prepared in Laemmli buffer, run on 10% SDS-PAGE, transferred, and probed for p-α-tubulin (Thr^{253}) and α-tubulin. Densitometric analysis was performed using ImageJ v.1.46, and data were plotted as the ratio between p-α-tubulin (Thr^{253}) and α-tubulin. Statistical significance of at least three experiments was determined using the Mann-Whitney test.

SUPPLEMENTARY MATERIALS

www.sciencesignaling.org/cgi/content/full/7/350/ra105/DC1

Fig. S1. Thr^{253}, Lys^{163}, and Lys^{164} are conserved in vertebrate α-tubulin.

Fig. S2. Specificity of the polyclonal antiserum recognizing α-tubulin phosphorylated on Thr^{253}.

Fig. S3. Models of known PKA substrates phosphorylated within sites in linear consensus motifs.

Table S1. Substrates of PKA obtained from PhosphositePlus modeled through homology modeling.

Table S2. RMSD calculation for PKA-docked models with linear consensus motifs, compared to the linear peptide and the nondocked substrate model.

Models S1. PDB files of the models of the three substrates with linear consensus motifs, three substrates with structurally formed consensus motifs, and the α-tubulin–PKC complex.

REFERENCES AND NOTES

1. B. E. Kemp, D. B. Bylund, T. S. Huang, E. G. Krebs, Substrate specificity of the cyclic AMP-dependent protein kinase. *Proc. Natl. Acad. Sci. U.S.A.* **72**, 3448–3452 (1975).
2. B. Kobe, T. Kampmann, J. K. Forwood, P. Listwan, R. I. Brinkworth, Substrate specificity of protein kinases and computational prediction of substrates. *Biochim. Biophys. Acta* **1754**, 200–209 (2005).
3. J. E. Hutti, E. T. Jarrell, J. D. Chang, D. W. Abbott, P. Storz, A. Toker, L. C. Cantley, B. E. Turk, A rapid method for determining protein kinase phosphorylation specificity. *Nat. Methods* **1**, 27–29 (2004).
4. Z. Songyang, S. Blechner, N. Hoagland, M. F. Hoekstra, H. Piwnica-Worms, L. C. Cantley, Use of an oriented peptide library to determine the optimal substrates of protein kinases. *Curr. Biol.* **4**, 973–982 (1994).
5. T. B. Trinh, Q. Xiao, D. Pei, Profiling the substrate specificity of protein kinases by on-bead screening of peptide libraries. *Biochemistry* **52**, 5645–5655 (2013).
6. A. N. Kettenbach, D. K. Schweppe, B. K. Faherty, D. Pechenick, A. A. Pletnev, S. A. Gerber, Quantitative phosphoproteomics identifies substrates and functional modules of Aurora and Polo-like kinase activities in mitotic cells. *Sci. Signal.* **4**, rs5 (2011).
7. N. M. Alto, S. H. Soderling, N. Hoshi, L. K. Langeberg, R. Fayos, P. A. Jennings, J. D. Scott, Bioinformatic design of A-kinase anchoring protein-in silico: A potent and selective peptide antagonist of type II protein kinase A anchoring. *Proc. Natl. Acad. Sci. U.S.A.* **100**, 4445–4450 (2003).
8. M. Hjerrild, A. Stensballe, T. E. Rasmussen, C. B. Kofoed, N. Blom, T. Sicheritz-Ponten, M. R. Larsen, S. Brunak, O. N. Jensen, S. Gammeltoft, Identification of phosphorylation sites in protein kinase A substrates using artificial neural networks and mass spectrometry. *J. Proteome Res.* **3**, 426–433 (2004).
9. J. Kitchen, R. E. Saunders, J. Warwicker, Charge environments around phosphorylation sites in proteins. *BMC Struct. Biol.* **8**, 19 (2008).
10. L. M. Iakoucheva, P. Radivojac, C. J. Brown, T. R. O'Connor, J. G. Sikes, Z. Obradovic, A. K. Dunker, The importance of intrinsic disorder for protein phosphorylation. *Nucleic Acids Res.* **32**, 1037–1049 (2004).
11. C. S. Gibbs, M. J. Zoller, Identification of electrostatic interactions that determine the phosphorylation site specificity of the cAMP-dependent protein kinase. *Biochemistry* **30**, 5329–5334 (1991).
12. P. Durek, C. Schudoma, W. Weckwerth, J. Selbig, D. Walther, Detection and characterization of 3D-signature phosphorylation site motifs and their contribution towards improved phosphorylation site prediction in proteins. *BMC Bioinformatics* **10**, 117 (2009).
13. A. Zanzoni, D. Carbajo, F. Diella, P. F. Gherardini, A. Tramontano, M. Helmer-Citterich, A. Via, Phospho3D 2.0: An enhanced database of three-dimensional structures of phosphorylation sites. *Nucleic Acids Res.* **39**, D268–D271 (2011).
14. N. Blom, S. Gammeltoft, S. Brunak, Sequence and structure-based prediction of eukaryotic protein phosphorylation sites. *J. Mol. Biol.* **294**, 1351–1362 (1999).
15. M. Su, K. Huang, C. Tung, Y. Lee, A new scheme to predict kinase-specific phosphorylation sites on protein three-dimensional structures, *Int. J. Biosci. Biochem. Bioinformatics* **3**, 473–478 (2013).
16. J. D. Blethrow, J. S. Glavy, D. O. Morgan, K. M. Shokat, Covalent capture of kinase-specific phosphopeptides reveals Cdk1-cyclin B substrates. *Proc. Natl. Acad. Sci. U.S.A.* **105**, 1442–1447 (2008).
17. L. N. Johnson, Substrates of mitotic kinases. *Sci. Signal.* **4**, pe31 (2011).
18. R. M. Biondi, A. R. Nebreda, Signalling specificity of Ser/Thr protein kinases through docking-site-mediated interactions. *Biochem. J.* **372**, 1–13 (2003).
19. J. A. Ubersax, J. E. Ferrell Jr., Mechanisms of specificity in protein phosphorylation. *Nat. Rev. Mol. Cell Biol.* **8**, 530–541 (2007).
20. J. R. Woodgett, K. L. Gould, T. Hunter, Substrate specificity of protein kinase C. Use of synthetic peptides corresponding to physiological sites as probes for substrate recognition requirements. *Eur. J. Biochem.* **161**, 177–184 (1986).
21. C. House, B. E. Kemp, Protein kinase C contains a pseudosubstrate prototope in its regulatory domain. *Science* **238**, 1726–1728 (1987).
22. H. M. Costa-Junior, N. M. Garavello, M. L. Duarte, D. A. Berti, T. Glaser, A. de Andrade, C. A. Labate, A. T. Ferreira, J. E. Perales, J. Xavier-Neto, J. E. Krieger, D. Schechtman, Phosphoproteomics profiling suggests a role for nuclear βIPKC in transcription processes of undifferentiated murine embryonic stem cells. *J. Proteome Res.* **9**, 6191–6206 (2010).
23. Z. Y. Zheng, Q. Z. Li, D. Y. Chen, H. Schatten, Q. Y. Sun, Translocation of phosphoprotein kinase Cs implies their roles in meiotic-spindle organization, polar-body emission and nuclear activity in mouse eggs. *Reproduction* **129**, 229–234 (2005).
24. J. Löwe, H. Li, K. H. Downing, E. Nogales, Refined structure of αβ-tubulin at 3.5 Å resolution. *J. Mol. Biol.* **313**, 1045–1057 (2001).
25. N. Narayana, S. Cox, S. Shaltiel, S. S. Taylor, N. Xuong, Crystal structure of a polyhistidine-tagged recombinant catalytic subunit of cAMP-dependent protein kinase complexed with the peptide inhibitor PKI(5–24) and adenosine. *Biochemistry* **36**, 4438–4448 (1997).
26. H. Jiang, D. Cheng, W. Liu, J. Peng, J. Feng, Protein kinase C inhibits autophagy and phosphorylates LC3. *Biochem. Biophys. Res. Commun.* **395**, 471–476 (2010).
27. Z. Xie, Z. Yang, K. M. Druey, Phosphorylation of RGS13 by the cyclic AMP-dependent protein kinase inhibits RGS13 degradation. *J. Mol. Cell. Biol.* **2**, 357–365 (2010).
28. J. L. Miller, H. Koc, E. C. Koc, Identification of phosphorylation sites in mammalian mitochondrial ribosomal protein DAP3. *Protein Sci.* **17**, 251–260 (2008).
29. T. P. Abeyweera, X. Chen, S. A. Rotenberg, Phosphorylation of α6-tubulin by protein kinase Cα activates motility of human breast cells. *J. Biol. Chem.* **284**, 17648–17656 (2009).
30. D. Schechtman, M. L. Craske, V. Kheifets, T. Meyer, J. Schechtman, D. Mochly-Rosen, A critical intramolecular interaction for protein kinase Cε translocation. *J. Biol. Chem.* **279**, 15831–15840 (2004).
31. E. Krieger, T. Darden, S. B. Nabuurs, A. Finkelstein, G. Vriend, Making optimal use of empirical energy functions: Force-field parameterization in crystal space. *Proteins* **57**, 678–683 (2004).
32. M. A. Larkin, G. Blackshields, N. P. Brown, R. Chenna, P. A. McGettigan, H. McWilliam, F. Valentin, I. M. Wallace, A. Wilm, R. Lopez, J. D. Thompson, T. J. Gibson, D. G. Higgins, Clustal W and Clustal X version 2.0. *Bioinformatics* **23**, 2947–2948 (2007).
33. D. Z. Rudner, R. Losick, A sporulation membrane protein tethers the pro-$ζ^K$ processing enzyme to its inhibitor and dictates its subcellular localization. *Genes Dev.* **16**, 1007–1018 (2002).

Acknowledgments: We would like to thank C. Adams (Stanford University Mass Spectrometry, Stanford, CA) for mass spectroscopic analysis; B. Malnic and R. Tonelli for cell lines; M. J. Manso Alves, W. Colli, R. I. Schumacher, H. Chaimovich, J. Kobarg, and A. Gordon for editing the manuscript; and F. Gueiros Filho for antibodies recognizing GFP and for inspiring discussions. **Funding:** H.M.C.-J. was a recipient of a FAPESP (Fundação de Amparo à Pesquisa do Estado de São Paulo) postdoctoral fellowship (2006/52062-6); M.L.D. and D.A.P. were recipients of FAPESP doctoral fellowships (2009/51337 and 2011/10321-3, respectively); D.A.B., a FAPESP postdoctoral fellowship (2010/15424-2); and M.-H.D., NIH grant HL52141. This research was supported by Brazilian agency grants FAPESP 2010/18640-8 and 2012/24154-4 to D.S. **Author contributions:** M.L.D., D.A.P., F.A.N.F., H.M.C.-J., M.-H.D., T.J.P.S., and P.S.L.d.O. performed the experiments. D.S., M.L.D., D.A.P., F.A.N.F., P.S.L.d.O., M.M.A.B., and J.X.-N. planned the experiments and analyzed the data. D.S., P.S.L.d.O., J.X.-N., M.M.A.B., and F.A.N.F. wrote the paper. All authors read and approved the paper. **Data and materials availability:** Three substrates with linear consensus motifs, three substrates with structurally formed consensus motifs, and the α-tubulin–PKC complex models (discussed in the manuscript) are available as PDB files in models S1.

Submitted 23 April 2014
Accepted 17 October 2014
Final Publication 4 November 2014
10.1126/scisignal.2005412
Citation: M. L. Duarte, D. A. Pena, F. A. N. Ferraz, D. A. Berti, T. J. P. Sobreira, H. M. Costa-Junior, M. M. A. Baqui, M.-H. Disatnik, J. Xavier-Neto, P. S. L. de Oliveira, D. Schechtman, Protein folding creates structure-based, noncontiguous consensus phosphorylation motifs recognized by kinases. *Sci. Signal.* **7**, ra105 (2014).

Protein folding creates structure-based, noncontiguous consensus phosphorylation motifs recognized by kinases

Mariana Lemos Duarte, Darlene Aparecida Pena, Felipe Augusto Nunes Ferraz, Denise Aparecida Berti, Tiago José Paschoal Sobreira, Helio Miranda Costa-Junior, Munira Muhammad Abdel Baqui, Marie-Hélène Disatnik, José Xavier-Neto, Paulo Sérgio Lopes de Oliveira and Deborah Schechtman

Sci. Signal. **7** (350), ra105.
DOI: 10.1126/scisignal.2005412

Origami-Like Substrate Recognition

Proteins fold into complex three-dimensional structures, yet most sites in proteins that are modified posttranslationally have been identified within short linear consensus motifs in the primary amino acid sequence. Duarte *et al*. found that kinases can recognize a consensus site that is formed by distinct noncontiguous parts of the folded substrate protein. They characterized in α-tubulin an example of what they termed a "structurally formed" consensus site, a threonine residue phosphorylated by a specific member of the protein kinase C (PKC) family, and then identified structurally formed consensus sites in other substrates of PKC and PKA (protein kinase A). Thus, researchers need to look beyond the linear sequence of the protein to its three-dimensional structure to identify all of the potential consensus phosphorylation sites in a protein.